COBEM 2021 26th International Congress of Mechanical Engineering
November 22-26, 2021, Virtual Congress, Brazil

COB-2021-0506
STUDY OF THE REGRESSION RATE IN HYBRID PROPELLANT ROCKET ENGINES USING A CFD TOOL

Matheus Henrique Pacheco
Federal University of ABC
pacheco.m@aluno.ufabc.edu.br
Loreto Pizzuti
Federal University of ABC
loreto.pizzuti@ufabc.edu.br

Abstract. *The use of Computational Fluid Dynamics (CFD) tools in the resolution of the flux field in combustion chambers of rocket engines with hybrid propellants has developed a lot in recent years. However, comprehensive models, which describe the complex interaction between the multiple relevant phenomena in the burning of these engines, are still limited and numerical simulations are often considered only as a qualitative tool in determining the thermo-fluid-dynamic field of the rocket. The present work proposal consists in a theoretical study of the regression rate of solid propellants in hybrid rocket engines, relating it to the main characteristic flow parameters. The simulations are performed using pre-defined mass flow rates of fuel and oxidant, gaseous component obeying the ideal gas law, chemical equilibrium within the pre-combustion chamber so that the gas remains with its initial composition without being affected by the nozzle, and calculating the rate of fuel mass flow as a function of wall heat flux. The main objective of this work is to test a commercial CFD tool - ANSYS Fluent - for the simulation of the regression process, using the steady-state non-viscous flow model, which numerically solves the equations for the conservation of mass, energy, and momentum. A simulation model was developed capable of representing the regression process in simple geometries of combustion chambers of rocket engines for hybrid propellant in non-reactive flow considering the paraffin pyrolysis temperature, which can be used as a basis for adding relevant phenomena such as combustion and radiation in hybrid rockets and for more complex geometries. As a secondary objective, it was tested the model's reproducibility on a second simple hybrid rocket engine geometry, contributing to the future definition of optimized geometries that help to reduce the loss of performance in fuel combustion through the analysis of the flow model worked here.*

Keywords: *regression rate, propulsion, hybrid rocket, numerical simulations.*

1. INTRODUCTION

Rocket propulsion systems are based on Newton's third law, which consists of the principle of action and reaction, in which it is stated that every action corresponds to a reaction of the same magnitude and direction, but in the opposite direction. Based on this, propulsion is the process of changing the state of motion of a body in relation to a given frame of reference.

Chemically propelled rocket engines can be divided into three classes according to the phase of the propellants involved. The first class is liquid propellant rocket engines, which generally consist of using two propellants, an oxidizer and a fuel, stored in the liquid phase, which react with each other in the combustion chamber. The second class is solid-propellant rocket engines, which use solid-phase propellants stored in the combustion chamber. Solid propellant has all the chemical elements for complete combustion (Sutton *et al*., 2001).

The third class, which is the class of interest in this project, is hybrid propellant rocket engines with its base model shown in Fig. 1. In this class, fuel and oxidant are in different phases, usually the gas phase oxidant and the solid phase fuel. These rocket motors have advantages over other classes, such as manufacturing safety, possibility of processing control and generally greater specific impulse than solid rocket motors (Sutton *et al*., 2001).

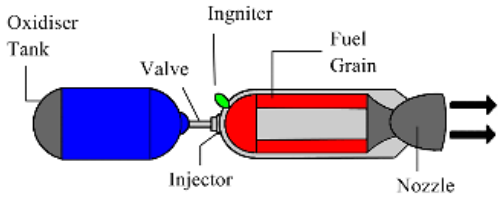

Figure 1. Hybrid propellant rocket engine model.

Several studies have been developed with the objective of performing the improvement and analysis of the hybrid propulsion system, more specifically, the analysis of the solid propellant regression rate. These studies are generally based on classical boundary layer analysis theories and were developed by Marxman, Majdalani and Vyas (Chiaverini *et al*., 2007). In general, a simplified correlation is used, presented in Eq. (1), in which the local instantaneous regression rate is a function of the local mass flow of the oxidant and the axial distance of port location, $\boldsymbol{x}$, in the form of power law.

$$\dot{r} = aG^n x^m \,, \tag{1}$$

In Eq. (1), $\dot{r}$ is the regression rate, a is a coefficient that can assume a constant value for a combination of propellants, G is the specific mass flow of the oxidant, given by Eq. (2), and the exponents n and m are numbers that in the classic model they have values of 0.8 and -0.2, respectively (Karabeyoglu *et al.*, 2005).

$$G = \frac{\dot{m}}{\frac{\pi D(t)^2}{2}} = \frac{\dot{m}}{\frac{\pi (D_0 + at^n)^2}{2}} \,, \tag{2}$$

Where $\dot{m}$ corresponds to the change in mass over time, $D(t)$ to the change in diameter over time, t to the elapsed time and D_0 to the initial diameter. However, this model does not take into account other factors that are relevant to the process, such as chamber pressure and radiation.

Chiaverini *et al* (2007) developed experimental studies similar to those of Marxman and added other factors for analysis, one of which was the quoted radiative flux. Motivated by this work, Sankaran and Merkle (1999) applied to this study the two-dimensional RANS model (Reynolds-Averaged Navier – Stokes), Eq. 3, which they developed for oxygen gas as oxidant and HTPB (hydroxyl-terminated polybutadiene) as fuel. They dealt with the limits of solid and gaseous phases with mass and energy balances at the interface, a fuel regression rate was implicitly obtained as part of the flux field solution and added the effects of thermal radiation, calibrated in order to follow the proposed model by Chiaverini *et al* (2007).

Navier–Stokes Equations:

$$\frac{\partial Q}{\partial t} + \frac{\partial E_i}{\partial x_i} = H + \frac{\partial V_i}{\partial x_i} \,, \tag{3}$$

Where:

$$Q = \begin{pmatrix} \rho \\ \rho u_j \\ e \\ \rho \kappa \\ \rho \epsilon \\ \rho Y_m \end{pmatrix}; E_i = \begin{pmatrix} \rho u_i \\ \rho u_i u_j + p_t \delta_{ij} \\ (e + p_t) u_i \\ p u_i \kappa \\ p u_i \epsilon \\ p u_i Y_m \end{pmatrix}; V_i = \begin{pmatrix} 0 \\ \tau_{ij} \\ u_j \tau_{\mathrm{ij}} + \mathrm{K} \frac{\partial T}{\partial x_i} \\ \mu_\kappa \frac{\partial \kappa}{\partial x_i} \\ \mu_\epsilon \frac{\partial \epsilon}{\partial x_i} \\ \rho D_m \frac{\partial Y_m}{\partial x_i} \end{pmatrix}$$

Since H is the vector that contains the source terms related to combustion, turbulence and radiation, ρ is the density (g/cm^3), u the axial component of the flow velocity (m/s), e the thickness of the boundary layer, κ the turbulent kinetic energy, ϵ the sidewall injection parameter given by U_w/U, ratio between the sidewall injection velocity and the tangential injection speed. The symbol μ indicates the dynamic viscosity (Ns/m^2), p the pressure (atm), K the thermal conductivity, D the mass diffusivity, T the temperature (K), x the longitudinal distance inside the combustion chamber, $m = 1, 2, \ldots, N-1$ where N is the total number of chemical species, Y_m is the mass fraction of the m-th species, the pressure $p_t = p + \frac{2}{3}\rho\kappa$, δ is the reciprocal of the Reynolds number and $\boldsymbol{\tau}$ is the viscous tension tensor that is given by

$$\tau_{ij} = \mu \left(\frac{\partial u_i}{\partial x_j} + \frac{\partial u_j}{\partial x_i} - \frac{2}{3}\delta_{ij} \frac{\partial u_l}{\partial x_l} \right) \,, \tag{4}$$

The equations related to the turbulence model that will be considered are

$$H_\kappa = \mu_t S - \frac{2}{3}\rho\epsilon - \frac{2\mu\kappa}{n^2} \,, \tag{5}$$

$$H_\epsilon = C_1 \mu_t (\epsilon/\kappa) S - \frac{2}{3} C_1 \rho \epsilon D - C_2 f_2 (2\rho\epsilon/\kappa^2) - \frac{2 f_1 \mu \epsilon}{n^2} \,, \tag{6}$$

Where:

$$\mu_t = C_\mu f_\mu \rho \kappa^2 / \epsilon \,, \tag{7}$$

$$S = \left[\frac{\partial u_i}{\partial x_j} + \frac{\partial u_j}{\partial x_i} + \frac{2}{3}\delta_{ij}\frac{\partial u_\kappa}{\partial x_\kappa}\right]\frac{\partial u_i}{\partial x_j} \,, \tag{8}$$

$$D = \frac{\partial u_i}{\partial x_i} \,, \tag{9}$$

Since C_μ, C_1 and C_2 are constants determined according to the defined flow model, for example, in the case of $\kappa - \epsilon$ model, so we have $C_\mu = 0.09$, $C_1 = 1.35$ and $C_2 = 1,8$, according to Chiaverini *et al* (2007).

Furthermore, it is possible to determine the heat flux of the gas phase through the Eq. (10) and the solid phase through the Eq. (11), (Mazzetti, 2013).

$$q_g = -\kappa_g \nabla T_g + \sum_{k=1}^{N\,S} h_i J_{i,g} \,, \tag{10}$$

$$q_s = -\kappa_s \nabla T_s \,, \tag{11}$$

Where q represents the heat flux considering conduction and convection, NS the number of species, h the enthalpy of the species and $\sum_{k=1}^{N\,S} J_i$ is the sum of the diffusion fluxes, with the g and s indices representing the gas phase and the solid phase, respectively.

The experiment of Favaró *et al.* (2013), using gaseous oxygen and HTPB as propellants, shows the effect caused by the presence of oxygen on the fuel surface, concluding that it is responsible for the increase in the pyrolysis rate (thermal decomposition) of the solid fuel. It was also found that the increase in the regression rate leads to an increase in the burn rate which can produce more heat transported back to the fuel surface, resulting in a higher surface temperature and a higher pyrolysis rate.

Recent works use several CFD platforms for modeling and analyzing the regression rate. Lazzarin *et al.* (2013) analyzed the regression rate through CFD simulations using oxygen gas as oxidant and HTPB and HDPE (High-Density Polyethylene) as fuel. The regression rate equation used is given by the Eq. (12) below:

$$\dot{r} = A \exp\left(-\frac{E_a}{nT_s R}\right) \,, \tag{12}$$

Where A is a constant in mm/s, R the universal gas constant in $J/(kg.mol.K)$, E_a is the activation energy of the process in J/mol and $\dot{r}$ is the average regression rate in mm/s.

In each step of the mentioned simulations, the meshes created were refined, seeking the convergence of the heat flux analyzed through the comparison in terms of pressure in the combustion chamber and heat flux to the walls. Lazzarin and coworkers concluded that CFD platforms present in the Ansys analysis software provide results coherent with the bibliography, although it is necessary to add more parameters, so that the presented error is reduced.

The present work fits into this scenario, as the non-reactive flow is studied - without considering the effects of radiation and combustion along the combustion chamber - in order to computationally simulate the fluid behavior taking into account the heat exchange present between the oxidizer and the paraffin. The objective of the present project is to develop a model using simple geometry and initial conditions to carry out the study of the regression rate in a rocket engine model with non-reactive flow aiming to build a simulation model so that other parameters can be added to the flow. From the addition of reactive flow in the studied base flow model, the regression rate analyzes will follow the line worked by Lazzarin *et al*. (2013) using Eq. 12 for this work.

2. PARAMETERS FOR THE SIMULATION

The geometry chosen to develop the present work is based on the project developed by Sporschill (2017), shown in Fig. 2, with its technical drawing shown in Fig. 3. The cylindrical symmetry factor presented by the solid was used in the geometry, so the simulations were performed faster and with the view facilitating the analysis.

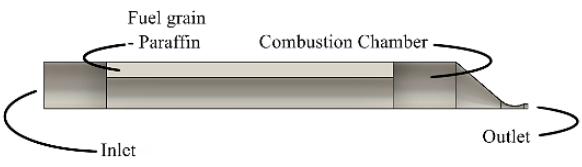

Figure 2. Simple geometry hybrid rocket engine.

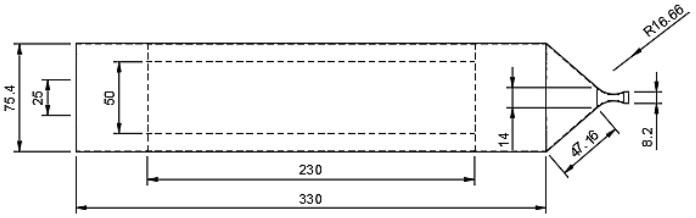

Figure 3. Technical drawing of the geometry.

The same procedure highlighted above on the use of symmetry in the first geometry, called geometry 01, was carried out for the second geometry, called geometry 02, based on Hui *et al*. (2014). Figure 4 shows the solid representation for the second geometry with the specified regions, while Fig. 5 is its technical drawing.

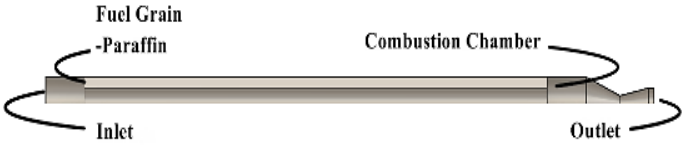

Figure 4. Second simple geometry hybrid rocket engine.

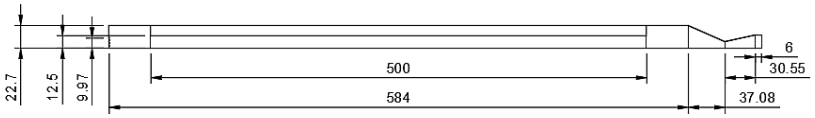

Figure 5. Technical drawing of the second geometry.

The analysis conditions defined for the computational simulations are based on the objective of the present project and therefore considering the following assumptions (Chiaverini *et al*, 2007):

- Homogeneous composition of the fluid;
- Heat exchange takes place only between the oxidizer and the paraffin;
- Solid and liquid phases add a negligible amount of mass to the system, that is, only the gaseous state of the components will be considered;
- The fluid obeys the Law of Ideal Gases;
- Flow is continuous;
- Non-reactive flow, so the effects of combustion and radiation are not considered;
- Thruster flow is constant;
- Transient effects will not be considered, the beginning and end of the flow are considered of short duration;
- Turbulent flow model → $\boldsymbol{\kappa - \epsilon}$,
- Within the pre-combustion chamber, the chemical balance is established and the gas composition does not change in the nozzle.

In addition, the boundary conditions are added to the mean values used in the works by Sporschill (2017), Banno *et. al.* (2019) e Mazzetti (2013):

- Gaseous oxygen inlet velocity of $33\ m/s$.
- Gaseous oxygen inlet temperature $300\ K$.
- Zero gauge pressure between inlet and outlet points.
- Paraffin pyrolysis temperature value $673\ K$.

The average values were adopted because the present work seeks to develop a non-reactive flow model so that in future projects the flow conditions with combustion can be added.

The meshes used in the simulations were created using the Ansys Mesh and the statistics of each mesh is shown in Tab. 1, where the values of nodes and the number of elements used are indicated.

Table 1. Grid statistics used in computational numerical analysis.

Statistics	**Geometry 01**	**Geometry 02**
Nodes	709 594	1 394 174
Elements	3 035 348	675 972

For the creation of meshes, the automatic method present in the software was used, in addition, the face meshing command was used for the side faces. To assess the quality of the mesh, two parameters were used, namely: skewness and element quality. The first one informs the degree of distortion of the element present in the mesh in relation to a normalized element, which can vary from 0 to 1, where the closer to zero, the smaller the distortion. The second provides a three-dimensional quality metric for the element, also ranging from zero to 1, and the closer to 1, the closer the proximity to a perfect cube.

These two parameters were applied in the second geometry in three meshes with different degrees of refinement, and the results are presented in Tab. 2.

Table 2. Analysis parameters for mesh quality in the second geometry.

Statistics	**Low Refinement**	**Intermediate Refinement**	**High Refinement**
Nodes	27 734	1 394 174	5 566 502
Elements	12 599	675 972	2 587 932
Element Size	5 mm	1 mm	0.6 mm
Skewness	0.23839	0.18799	0.17473
Element Quality	0.84197	0.86552	0.87268

For the simulation processes to be carried out, in order to reduce the computational requirement, the mesh with intermediate refinement was used, considering that both analyzed parameters present average values close to the values of the more refined mesh. This result was extended to the first geometry used.

In addition, it was necessary to add the properties of paraffin, presented in Tab. 3, to Fluent - Ansys, based on the work of Banno *et al.* (2019) and Mahottamananda *et. al.* (2020).

Table 3. Solid fuel data used in simulations.

Solid fuel data	
Property	**Value**
Fuel density	$900 \frac{kg}{m^3}$
Specific heat	$2800 \frac{J}{kgK}$
Thermal conductivity	$0.25 \frac{W}{mK}$

3. RESULTS AND DISCUSSIONS

The obtained simulation results are shown in Fig. 6, for geometry 01, and in Fig. 7, for geometry 02. Both were performed using the same input parameters described, using non-reactive flow and with heat exchange only between the gas and the paraffin. The chamber has being removed from the process as it was considered adiabatic, not relevant in this analysis. The oxidant flows from the right to the left side in both figures.

In Fig. 6 it is possible to notice that in the boundary layer region, where it is possible to analyze the regression rate, the temperature ranges between the values of $375\ K$ and $450\ K$, while for the second geometry, shown in Fig. 7, the

temperature ranges between 375 K and 486 K. This difference is due to the longer grain of geometry 02, so that a larger surface area is available for heat exchange between the components.

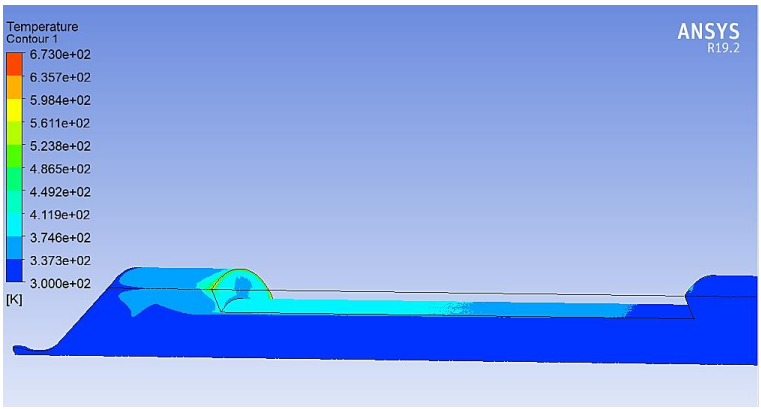

Figure 6. Computer simulation for analysis of the regression rate in geometry number 1.

In addition, in geometry 02, the temperature change layer along the flow presented greater thickness, thus, in addition to the oxidant reaching higher temperatures, this temperature also spreads more to the central region of the chamber.

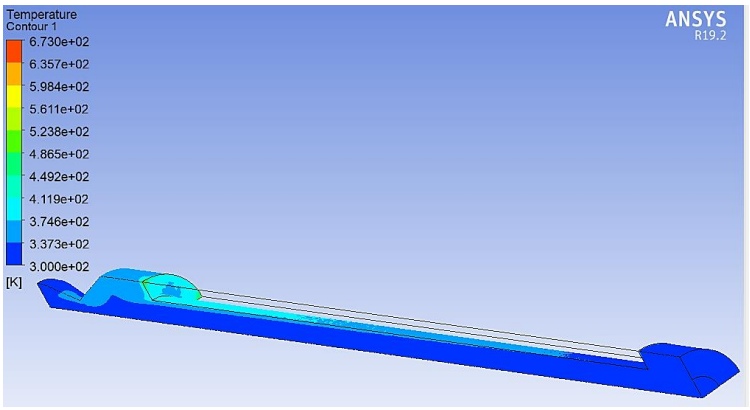

Figure 7. Computer simulation for analysis of the regression rate in geometry number 2.

In both cases, it is noted that the oxygen gas temperature remains almost constant at 300 K, the temperature at the inlet region, until the oxidant meets the paraffin. This result indicating the combustion chamber as adiabatic.

The exit temperature of the fluid is 300 K, this due to the high speed of the oxidant inlet, showing that the heat exchange present between the elements does not significantly affect the temperature of the fluid in the central region. It will be affected more visibly through the inclusion of phenomena such as combustion and radiation, that is, through the analysis of a reactive flow that can be added to the model in the future works. The flux temperature variation along the second geometry, shown in Fig. 9, matches the Streamline shown in Fig. 8, which has the characteristic of considering all domains starting in the inlet region ending in the outlet region and Sampling being Equally Spaced.

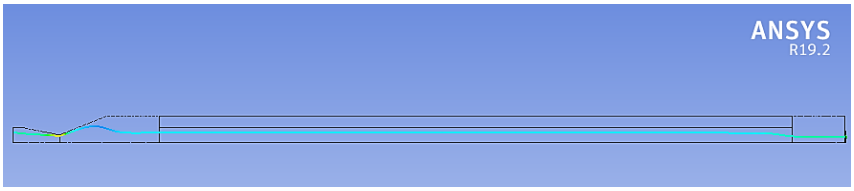

Figure 8. Streamline in geometry number 2.

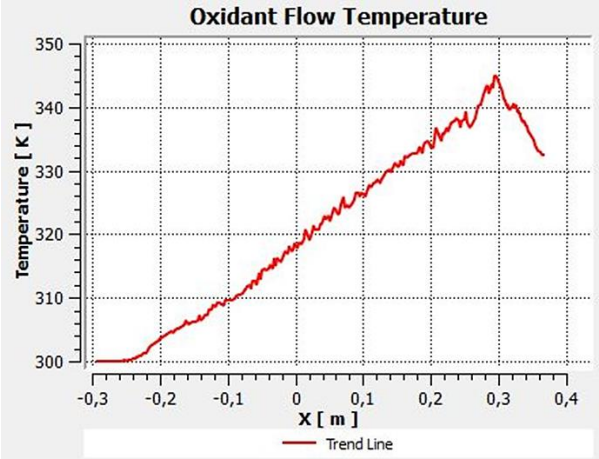

Figure 9. Temperature variation of the flow along the second geometry.

Considering geometry 02, Fig. 10 shows the flow velocity of the oxidant inside the combustion chamber considering the contact with the paraffin wax.

Figure 10. Flow velocity along the second geometry.

Note that, at the chamber inlet the oxidizer flow velocity changes when it comes into contact with the fuel grain, reaching a mean velocity of 8.4 m/s. When advancing in the horizontal direction towards the exit of the chamber, the flow velocity increases, reaching the value of 25.44 m/s at the end of the grain. Analyzing the velocity profile in vertical sections of the chamber, it is possible to observe the increase of the boundary layer thickness and the flow velocity is also increased, until in the central region it appears with an approximate value of 30 m/s.

Mazzetti (2013) analyzes the transverse velocity profile of laminar and turbulent flows, presenting results similar to those shown in Fig. 10, thus validating the results. The results presented by the flow velocity not taking into account the presence of turbulence are qualitatively satisfactory when compared to the results presented by Mazzetti for the same model, with the boundary conditions used and the developed model can be considered capable of correctly solving the flow adopted.

It is interesting to analyze the velocity contour using the streamlines, as in this way it is possible to observe the vortexes more clearly, as shown in Fig. 11 so that all the flow is shown and in Fig. 12 focusing on the exit region.

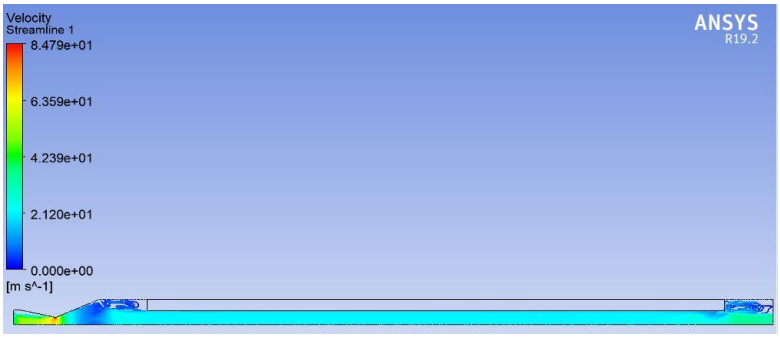

Figure 11. Fluid flow velocity along the second geometry.

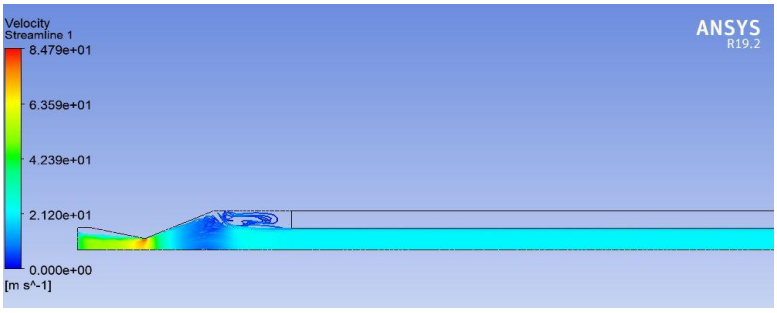

Figure 12. Fluid flow in geometry 2 with focus on end region.

A similar behavior is observed in the work carried out by Mazzetti (2013) for non-reactive flow with turbulent and laminar flow thus validating the simulation.

4. CONCLUSION

Hybrid rocket engines are a class of rockets that can feature oxidizer in the gas phase and paraffin as the solid part. The analysis of this model is important not only for its safer use compared to solid and liquid propulsion engines, but also because they can generate relevant specific impulse and thrust. The objective of the present project was to develop and validate a simulation model using simple geometry and initial conditions to carry out the study of the regression rate in a rocket engine model with non-reactive flow. A $\kappa - \epsilon$ turbulent flow model is considered.

The developed model showed to be efficient in the flow simulation, as it does not exhibit heat exchange in regions determined as adiabatic, like the symmetry walls used for the solid cuts and the contact regions of the elements with the combustion chamber. It presents temperatures coherent with the parameters of thermal conductivity and paraffin pyrolysis temperature. In addition, the flow velocity profile has been validated against some of the available literature.

The present work should serve as a basis for works that seek a more detailed analysis of the regression rate with increasing accuracy and model complexity. One suggestion is the study of reactive flow with the analysis of both the effects of combustion and radiation on the fuel regression rate.

5. ACKNOWLEDGEMENTS

The authors gratefully acknowledge the financial support of a scholarship provided by CNPq (*Conselho Nacional de Pesquisa* - National Research Council) through the process 134007/2020-4 and UFABC (Federal University of ABC).

6. REFERENCES

Banno, A., Wada, Y., Mishima, Y., Tsugoshi, T., Kato, N., Hori, K., Nagase, R., 2019. *Influence of Heating Rate on Pyrolysis Process of Paraffin Oil for Rocket Fuel.* 8th European Conference for Aeronautics And Space Sciences (EUCASS), DOI: 10.13009/EUCASS2019-618.

Chiaverini, and M.J., Kou, K.K., 2007. *Fundamentals of Hybrid Rocket Combustion and Propulsion*. American Institute Of Astronautics And Aeronautics, Inc., Vol. 218.

Favaró, F. M., Manzoni, M., Coronetti, A.,Deluca, L.T. and Sirignano, W.A., 2013. *Solid Fuel Regression Rate Modeling for Hybrid Rockets.* European Conference for Aeronautics and Space Sciences (EUCASS).

Hui, T., Yijie, L., Peng, Z., 2014. *Transient Simulation of Regressionrate on Thrust Regulation Process in Hybrid Rocketmotor*. Chinese Journal Of Aeronautics, 27(6): 1343–1351.

Karabeyoglu, M.A., Cantwell, B.J., and Zilliac, G., 2005. *Development of Scalable Space-time Averaged Regression Rate Expressions for Hybrid Rockets*. 41st AIAA/ASME/SAE/ASEE Joint Propulsion Conference & Exhibit.

Lazzarin, M., Pavarin, D., Barato, F. and Battella, A., 2013. *CFD Simulation of Regression Rate in Hybrid Rockets.* Journal of Propulsion and Power 29(6).

Mahottamananda, S.N., Kadiresh, P.N., 2020. *Mechanical Characteristics of Paraffin Wax-HTPB Based Hybrid Rocket Fuel*. DOI: 10.1007/978-981-15-4756-0_9.

Mazzetti, A., 2013. *Numerical Modeling and Simulations of Combustion Processes in Hybrid Rocket Engines*. Politecnico Di Milano, Mathematics Department "F. Brioschi", Doctoral Programme in Mathematical Models and Methods in Engineering.

Pal, Y., Raja, A., Gopalakrishnan, K., 2020. *Theoretical and Experimental Heat of Combustion Analysis of Paraffin-Based Fuels as Preburn Characterization for Hybrid Rocket.* J. Aerosp. Technol. Manag., São José dos Campos, v12, e4520.

Sporschill, G., 2017. *Numerical Approach of a Hybrid Rocket Engine Behaviour - Modelling the Liquid Oxidizer Injection Using a Lagrangian Solver.* Onera – Multi-Physics for Energetics Department.

Sutton, G.P., and Biblarz, O., 2001. *Rocket Propulsion Elements*. John Wiley & Sons, Inc., Vol. 9, 2017.

7. RESPONSIBILITY NOTICE

The authors are the only responsible for the printed material included in this paper.